

A Report
on
Shape from Shading - Theory and Applications

By
Balaje K
Sanath Keshav

**Tata Institute of Fundamental Research - Center
for Applicable Mathematics**



July 2016

Acknowledgements

We would like to sincerely thank Prof. G.D.Veerappa Gowda for providing us with an opportunity to work at TIFR-CAM on this project. We thank Dr. Aekta Aggarwal for providing us with valuable inputs, suggestions and tips throughout the Internship.

We thank our parents for providing us with constant support and encouragement which helped us throughout this project. We thank the Almighty, without which none of this would have been possible.

Once again we thank them all.

List of Figures

1.1	Shape from Shading : The <i>ground truth</i> is the original object and SfS attempts to reconstruct it, just from knowing the <i>Intensity map</i>	5
3.1	Orthographic camera model	19
4.1	a) Orthographic vs b) Perspective : Number of Singular Points	22
4.2	Perspective Projection Model	23
6.1	Viscosity Soution of the 1D Eikonal Equation	32
6.2	Evolution of solution to the Eikonal Equation. The steady state condition is taken as $\ U^{n+1} - u^n\ < \epsilon = 10^{-16}$	33
6.3	Solution of 2D Eikonal Equation	34
6.4	Immersed Circle	35
6.5	Inout Matrix for 10×10 mesh	35
6.6	Solution in a circular domain	36
6.7	Other Domains	37
6.8	Synthetic Test Vase	37
6.9	Reconstruction of the Synthetic Test Vase	38
6.10	Reconstruction using Perspective Model by Prados [2]	39
6.11	Time evolution of Mozart's Face	40
6.12	Real Life Reconstructions	41

Contents

1	Introduction	5
2	Viscosity Solutions to Hamilton Jacobi Equations	7
2.1	Hamilton Jacobi Equations	7
2.2	Well Posedness	7
2.3	Viscosity Solutions	8
2.3.1	Need for Viscosity Solutions	8
2.3.2	Viscosity Solutions	8
2.4	Legendre Transform	12
2.4.1	Classical Definition	12
2.4.2	Generalized Legendre Transform	13
2.5	Coercivity and Legendre Transform	14
2.6	Compatibility Condition	15
2.6.1	Viscosity Subsolution Criterion	15
2.6.2	Compatibility condition using Legendre Transform	16
2.7	Comparison Theorem	17
2.7.1	Classical Comparison Theorem	17
2.7.2	Comparison Theorem	17
3	Orthographic Shape from Shading	19
3.1	Mathematical formulation of the Model	19
3.2	Problem of Uniqueness	20
4	Perspective Shape from Shading	22
4.1	Mathematical Model	22
4.2	Existence and Uniqueness	24
5	Numerical Schemes	26
5.1	Hyperbolic Conservation Laws	26
5.2	Numerical Schemes for Hyperbolic Conservation Laws	28
5.2.1	The Godunov Scheme	28
5.2.2	Lax-Friedrich Scheme	29
5.3	Godunov Scheme for the Eikonal Equation	29

6	Numerical Experiments	31
6.1	1D Eikonal Equation	31
6.2	2D Eikonal Equation	32
6.3	Immersed Boundary Method for 2D Eikonal Equations	32
6.3.1	Results	34
6.4	Orthographic Projection	37
6.5	Perspective Projection Model	38
7	Conclusion	42

Chapter 1

Introduction

Shape from Shading (SfS) is a 3D image reconstruction technique, in which the shape of a 3D object (output) is retrieved from a 2D image (input). The 2D image is a light intensity map of the 3D object, which is a grayscale image. The intensity map is obtained by flashing light over the object from a particular point (known *a priori*) to illuminate the object. Then a mathematical model is constructed to relate the pixel intensity in the input image to obtain the depth information of the 3D surface. Figure (1.1) gives a flow chart of the process in SfS.

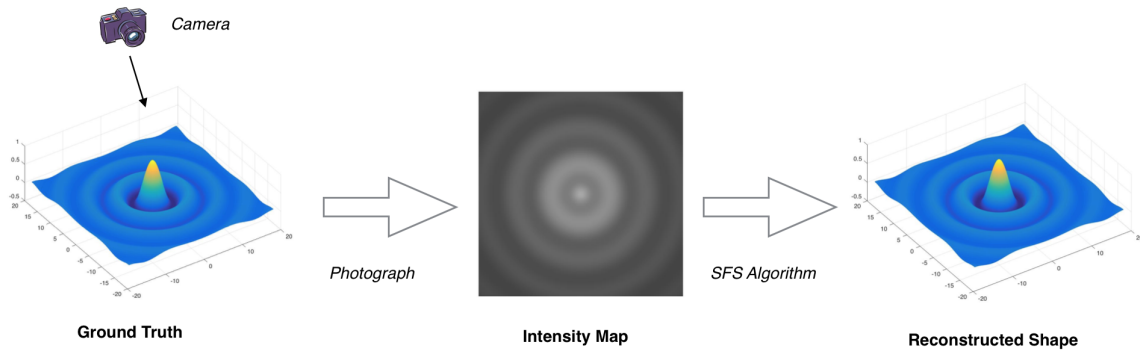


Figure 1.1: **Shape from Shading** : The *ground truth* is the original object and SfS attempts to reconstruct it, just from knowing the *Intensity map*

The relation between the intensity of a pixel and the height of our reconstructed surface is given by a PDE. K.P.Horn[9] has given an eikonal equation type approach to formulate the Shape from Shading problem. This is known as the **orthographic projection model**. Rouy and Tourin[18] came up with a viscosity solution approach to the model, and constructed an upwind type numerical scheme to solve the Eikonal type equation. Though this model was simple and effective, it suffered from a disadvantage because of singular points (More on singular points will be discussed in the coming chapters), where uniqueness of the solution is lost.

Prados and Faugeras[2] came up with a much more realistic model that takes care of this difficulty. To solve the resulting PDE, Prados and Faugeras[3] formulates a minimization approach, although solving the PDE using numerical techniques works as good. In this work, we present a numerical method to solve the PDE that arises due to Prados's work without using the minimization approach. Some applications of shape from shading can be found in [3]

This report is divided into 6 chapters. Chapter 2 introduces the reader to Hamilton Jacobi Equations (HJE), which is the backbone of Shape from Shading. This chapter discusses the need for viscosity solutions, and some existence, uniqueness results. Chapter 3 deals with the development of Orthographic Projection Model and discusses the notion of singular points and some ways to overcome the problem. Chapter 4 discusses the Perspective Projection approach to SfS problems and presents some existence and uniqueness results. Chapter 5 deals with the construction of some numerical schemes to solve the Eikonal Equation in a variety of domains, using the immersed boundary method. Numerical schemes to solve the SfS problems are discussed and the stability of these schemes are explained. Chapter 6 presents the results of some numerical experiments that were conducted on a variety of synthetic images to illustrate SfS.

Chapter 2

Viscosity Solutions to Hamilton Jacobi Equations

2.1 Hamilton Jacobi Equations

A Hamilton Jacobi equation (HJE) is a non-linear Partial Differential Equation of the form

$$H(\mathbf{x}, u(\mathbf{x}), Du(\mathbf{x})) = 0 \text{ in } \Omega \quad (2.1)$$

$$u(\mathbf{x}) = \varphi(\mathbf{x}) \text{ on } \partial\Omega \quad (2.2)$$

where $\mathbf{x} = (x_1, \dots, x_n) \in \mathbb{R}^n$, $u(\mathbf{x}) \in \mathbb{R}$ and $Du(\mathbf{x})$ is the first order derivative of u in \mathbb{R}^n , defined by,

$$Du(\mathbf{x}) = \left(\frac{\partial u}{\partial x_1}, \dots, \frac{\partial u}{\partial x_n} \right)^T \quad (2.3)$$

The function $H(\mathbf{x}, u(\mathbf{x}), Du(\mathbf{x})) : \Omega \times \mathbb{R} \times \mathbb{R}^n \rightarrow \mathbb{R}$ is known as the Hamiltonian. $u(\mathbf{x})$ is our unknown function. The problem defined by (2.1)-(2.2) is known as the Dirichlet Boundary Value Problem (BVP). The other class of problem, known as the Cauchy Problem is given by,

$$\frac{\partial u}{\partial t} + H(\mathbf{x}, t, u(\mathbf{x}, t), Du(\mathbf{x}, t)) = 0 \quad \text{in } \Omega \times]0, T] \quad (2.4)$$

$$u(\mathbf{x}, t) = \varphi(\mathbf{x}, t) \quad \text{on } \partial\Omega \times]0, T] \quad (2.5)$$

$$u(\mathbf{x}, 0) = u_0(\mathbf{x}) \quad \text{in } \Omega \quad (2.6)$$

The function $u_0(\mathbf{x})$ is known as the initial condition. These types of PDEs were investigated by the Irish Mathematician William Rowan Hamilton[6, 7].

2.2 Well Posedness

According to Hadamard[5], a mathematical model has to be well posed. A well posed problem has the following properties,

1. **Existence** - There exists a solution to the problem.

2. **Uniqueness** - There exists atmost one solution to the problem.

3. **Stability** - The solution depends continuously on the data.

The existence of a solution to the HJE can be assured if we enlarge the space of functions under consideration. For example, as we will see soon enough, the Eikonal Equation has a solution in C^0 , the space of continuous functions, but not in C^1 , the space of continuously differentiable functions. The uniqueness of a problem is normally obtained by supplying additional information like initial/boundary data, so that we can capture the physically relevant solution. Stability is an important criterion while constructing the numerical schemes, as a small perturbation in the initial data should produce small changes in the solution to the PDE. This situation becomes relevant when we tend the mesh size $h \rightarrow 0$, the computed solution should converge to the exact solution of the PDE[13].

2.3 Viscosity Solutions

2.3.1 Need for Viscosity Solutions

The Hamilton Jacobi Equations are normally not well-posed under the classical solution approach. The properties of existence and uniqueness in the classical sense are no longer satisfied.

For example, when we consider solving the Eikonal Equation in 1D,

$$|u'| = 1 \quad \text{in } \Omega \equiv (0, 1) \quad (2.7)$$

$$u = 0 \quad \text{on } \partial\Omega \equiv \{0, 1\} \quad (2.8)$$

which is a HJE, it can be shown that the solution to the problem does not exist in C^1 . This can be easily proved using contradiction. Consider that we are looking for a solution $u \in C^1$. As we have, $u(0) = u(1) = 0$, by Rolle's Theorem, $\exists x_0 \in (0, 1)$ such that $u'(x_0) = 0$, which contradicts (2.7). So $u \notin C^1$. This shows that, we have solutions that are not differentiable at certain points on the domain but $u \in C^0$. Such solutions satisfy the PDE in a “weaker” sense and hence are called **weak solutions**.

One can see that $u^+(x) = \frac{1}{2} - |\frac{1}{2} - x|$ is a *weak* solution to the Dirichlet Problem (2.7)-(2.8). But we can see that $u^-(x) = -u^+(x)$ is a solution to the problem as well. Hence, the classical approach becomes insufficient to guarantee a unique solution to the Dirichlet Problem.

2.3.2 Viscosity Solutions

P.L.Lions and M.G.Crandall[1] came up with a setting to obtain the existence and uniqueness properties for the Hamilton Jacobi Equation. They are known as **viscosity solutions**. The term **viscosity** is used because solution to the HJE is obtained by adding a viscosity term ϵu_{xx} to the HJE and letting $\epsilon \rightarrow 0$ to obtain the solution to our original PDE. Before we see how to obtain the viscosity solutions, we must find a way to deal with the non-differentiable points in C^0 solutions. For this we define **super differentials** and **sub differentials**. Super- and sub-differentials replaces the

classical derivatives at non-differentiable points in the functions and are equivalent to the classical definition at differentiable points.

For the following HJE,

$$H(\mathbf{x}, \nabla u(\mathbf{x})) = 0 \quad \text{in } \Omega \quad (2.9)$$

$$u(\mathbf{x}) = \varphi(\mathbf{x}) \quad \text{on } \partial\Omega \quad (2.10)$$

Definition 2.3.1 A continuous function $u \in C^0$ is a viscosity solution to the HJE, if it satisfies the following conditions

1. **Viscosity Subsolution** : For any test function $\varphi \in C^1$, if \mathbf{x}_0 is the local maximum of $u - \varphi$, then

$$H(\mathbf{x}_0, \nabla u(\mathbf{x}_0)) \leq 0$$

2. **Viscosity Supersolution** : For any test function $\varphi \in C^1$, if \mathbf{x}_0 is the local minimum of $u - \varphi$, then

$$H(\mathbf{x}_0, \nabla u(\mathbf{x}_0)) \geq 0$$

An alternate, but an equivalent definition of the same is given using sub- and super- differentials.

Definition 2.3.2 A continuous function $u \in C^0$ is a viscosity solution to the HJE, if it satisfies the following conditions

1. **Viscosity Subsolution** : $H(\mathbf{x}, p) \leq 0$ for all $\mathbf{x} \in \mathbb{R}^n$ and $p \in D^+u$
2. **Viscosity Supersolution** : $H(\mathbf{x}, q) \geq 0$ for all $\mathbf{x} \in \mathbb{R}^n$ and $q \in D^-u$

where,

$$D^+u = \left\{ p \in \mathbb{R}^n \mid \limsup_{y \rightarrow x} \frac{u(y) - u(x) - p \cdot (y - x)}{|y - x|} \leq 0 \right\} \quad (2.11)$$

$$D^-u = \left\{ q \in \mathbb{R}^n \mid \liminf_{y \rightarrow x} \frac{u(y) - u(x) - q \cdot (y - x)}{|y - x|} \geq 0 \right\} \quad (2.12)$$

The sets D^+u and D^-u are known as the super- and sub-differentials, respectively. A collection of some properties of sub- and super-differentials are listed below. Refer [11] for more details.

1. D^+u and D^-u are convex subsets of \mathbb{R}^n .
2. If u is differentiable at any point \mathbf{x} , then

$$\{Du(\mathbf{x})\} = D^+u(\mathbf{x}) = D^-u(\mathbf{x})$$

3. If for some \mathbf{x} , both D^+u and D^-u are non-empty,

$$\{Du(\mathbf{x})\} = D^+u(\mathbf{x}) = D^-u(\mathbf{x})$$

4. $D^+(\alpha u)(\mathbf{x}) = \alpha D^+u(\mathbf{x})$, $\alpha > 0$

$$5. D^+(\alpha u)(\mathbf{x}) = \alpha D^-u(\mathbf{x}), \quad \alpha < 0$$

$$6. D^+(u + \varphi)(\mathbf{x}) = D^+u(\mathbf{x}) + D\varphi(\mathbf{x}), \quad \text{if } \varphi \in C^1$$

$$7. D^+u_\alpha(\mathbf{x}) = \alpha D^+u(\mathbf{x}) + (1 - \alpha)D\varphi \quad \text{where,} \quad u_\alpha = \alpha u(\mathbf{x}) + (1 - \alpha)\varphi(\mathbf{x})$$

The following example illustrates the procedure for calculating the super and sub-differentials of a function in 1D. We do this for $u^+(x) = 1 - |x|$ and use them to isolate the viscosity solution of the following Eikonal equation with Dirichlet boundary data. (In fact we show that $u^+(x)$ is the viscosity solution to our Dirichlet BVP).

$$|u'| = 1 \quad \text{in } \Omega \equiv (-1, 1) \quad (2.13)$$

$$u = 0 \quad \text{on } \partial\Omega \equiv \{-1, 1\} \quad (2.14)$$

Example 2.3.1 *Super and sub differential of $u(x) = 1 - |x|$*

Super Differential D^+u :

We consider the case only when $x = 0$, as $x = 0$ is the only non-differentiable point. The classical definition of the derivative holds for the case $x \neq 0$ as the function is differentiable at these points. For full details, refer [11]

1. $x = 0$

$$\bullet \ y \geq 0 \implies |y| = y \implies 1 - |y| = 1 - y$$

$$\iff \limsup_{y \rightarrow x} \frac{u(y) - u(x) - p(y - x)}{|y - x|} \leq 0 \quad (2.15)$$

$$\iff \limsup_{y \rightarrow 0} \frac{(1 - y) - 1 - p(y - 0)}{|y - 0|} \leq 0 \quad (2.16)$$

$$\iff \limsup_{y \rightarrow 0} \frac{-y - py}{y} \leq 0 \quad (2.17)$$

$$\text{As } y \geq 0 \iff -y - py \leq 0 \implies y(1 + p) \geq 0 \implies p \geq -1$$

$$\bullet \ y \leq 0 \implies |y| = -y \implies 1 - |y| = 1 + y$$

$$\iff \limsup_{y \rightarrow x} \frac{u(y) - u(x) - p(y - x)}{|y - x|} \leq 0 \quad (2.18)$$

$$\iff \limsup_{y \rightarrow 0} \frac{(1 + y) - 1 - p(y - 0)}{|y - 0|} \leq 0 \quad (2.19)$$

$$\iff \limsup_{y \rightarrow 0} \frac{y - py}{-y} \leq 0 \quad (2.20)$$

$$\text{As } -y \geq 0 \iff y - py \leq 0 \implies y(1 - p) \leq 0 \implies p \leq 1$$

From the two cases, we conclude that when $x = 0$, $p \in [-1, 1]$

2. $x < 0$, we have from the classical definition $p = \{1\}$

3. $x > 0$, we have from the classical definition $p = \{-1\}$

Hence from the above steps, we conclude that the super differential of $1 - |x|$ is

$$D^+u = \begin{cases} 1 & x \leq 0 \\ [-1, 1] & x = 0 \\ -1 & x \geq 0 \end{cases} \quad (2.21)$$

Following the same procedure, we can find the sub-differential of $1 - |x|$.

Sub Differential D^-u

1. $x = 0$

$$\bullet \ y \geq 0 \implies |y| = y \implies 1 - |y| = 1 - y$$

$$\iff \liminf_{y \rightarrow x} \frac{u(y) - u(x) - p(y - x)}{|y - x|} \geq 0 \quad (2.22)$$

$$\iff \liminf_{y \rightarrow 0} \frac{(1 - y) - 1 - p(y - 0)}{|y - 0|} \geq 0 \quad (2.23)$$

$$\iff \liminf_{y \rightarrow 0} \frac{-y - py}{y} \geq 0 \quad (2.24)$$

$$\text{As } y \geq 0 \iff -y - py \geq 0 \implies y(1 + p) \leq 0 \implies p \leq -1$$

$$\bullet \ y \leq 0 \implies |y| = -y \implies 1 - |y| = 1 + y$$

$$\iff \liminf_{y \rightarrow x} \frac{u(y) - u(x) - p(y - x)}{|y - x|} \geq 0 \quad (2.25)$$

$$\iff \liminf_{y \rightarrow 0} \frac{(1 + y) - 1 - p(y - 0)}{|y - 0|} \geq 0 \quad (2.26)$$

$$\iff \liminf_{y \rightarrow 0} \frac{y - py}{-y} \geq 0 \quad (2.27)$$

$$\text{As } -y \geq 0 \iff y - py \geq 0 \implies y(1 - p) \geq 0 \implies p \geq 1$$

From the two cases, we conclude that when $x = 0$, $p = \phi$

2. $x < 0$, we have from the classical definition $p = \{1\}$

3. $x > 0$, we have from the classical definition $p = \{-1\}$

Hence from the above steps, we conclude that the sub differential of $1 - |x|$ is

$$D^-u = \begin{cases} 1 & x \leq 0 \\ \emptyset & x = 0 \\ -1 & x \geq 0 \end{cases} \quad (2.28)$$

With the super- and sub- differentials in our hand, we now see how this can be used to pick out the unique viscosity solution of the Eikonal equation. Let us consider $u(x) = 1 - |x|$ and the convex Hamiltonian $H(x, p) = |p| - 1$ for the Eikonal equation. Now we have from 2.21

$$|p| \leq 1 \implies |p| - 1 \leq 0 \quad \forall p \in D^+u \quad (2.29)$$

$$\implies H(x, p) = |p| - 1 \leq 0 \quad \forall p \in D^+u \quad (2.30)$$

Thus, the viscosity sub-solution condition is satisfied. Since $D^-u = \emptyset$ for $x = 0$, the super-solution condition is satisfied trivially. Thus $u(x) = 1 - |x|$ is a **viscosity solution** to the Eikonal equation with homogeneous Dirichlet boundary conditions.

But on the other hand, $u(x) = |x| - 1$ is **not a viscosity solution** to the Eikonal Equation with the convex Hamiltonian $H(x, p) = |p| - 1$, as the super-solution condition $H(x, p) \geq 0$ is not satisfied by the sub-differential of $|x| - 1$. But $u(x) = |x| - 1$ is the viscosity solution to the Eikonal equation with non-convex Hamiltonian $H(x, p) = 1 - |p|$ and $u(x) = 1 - |x|$ is not. This shows that the viscosity solution is dependent on the nature of Hamiltonian used and *changing the Hamiltonian does not preserve the Viscosity Solution*.

2.4 Legendre Transform

A Legendre Transform is a peculiar transformation which connects the Hamiltonian and Lagrangian approaches in physics. Legendre transform can be viewed as a means to express information in an alternate and a simpler way. Zia et. al. in their paper titled “Making sense of the Legendre Transform” [17] presented a way to see Legendre transform as a powerful mathematical tool. They explain the origins of the Legendre Transform and its applications to various problems in Physics. In this report, we see how the Legendre Transform is defined in the classical sense and to extend the same to the viscosity setting.

2.4.1 Classical Definition

In this section, we see how the Legendre Transform is defined in the classical sense. We assume a differentiable function $f : \mathbb{R}^n \rightarrow \mathbb{R}$ and its gradient $\nabla f \in \mathbb{R}^n$. Writing the gradient as a map

$$\nabla : \mathbb{R}^n \rightarrow \mathbb{R}^n \quad (2.31)$$

Now we have the composite mapping,

$$\nabla f : \mathbb{R}^n \xrightarrow{f} \mathbb{R} \xrightarrow{\nabla} \mathbb{R}^n \quad (2.32)$$

Now we are interested in defining an inverse map $(\nabla f)^{-1}$ for the above composite mapping. Now we need to find the value of x that satisfies $s = \nabla f(x)$. Let us call that ∇h , so that $x = \nabla h(s)$.

The procedure for finding out h is illustrated below in 1D.

$$\begin{aligned}
\Rightarrow \quad \frac{df}{dx} &= s \\
\Rightarrow \quad df &= sdx \\
\Rightarrow \quad df &= d(sx) - xds \\
\Rightarrow \quad df - d(sx) &= -xds \\
\Rightarrow \quad d(sx - f) &= xds \\
\Rightarrow \quad \frac{d}{ds}(sx - f) &= x
\end{aligned} \tag{2.33}$$

From this we get $h(s) = sx(s) - f(x(s))$. This is defined as the Legendre Transform of the function $f(x)$.

Definition 2.4.1 Classical Legendre Transform of $f(x)$

Let $x \in \mathbb{R}^n$ and $S \subset \mathbb{R}^n$, and $s \in S$. The mapping $h(s) : S \rightarrow \mathbb{R}$,

$$h(s) = \langle x, s \rangle - f(x(s)) \tag{2.34}$$

is known as the Legendre Transform of $f(x)$.

This definition assumes that the function $f(x)$ is differentiable. In the next subsection we will see how to extend the Legendre Transform to a non-differentiable function like $|x|$. We will also see how the Legendre transform is used to define the compatibility condition on the boundary data to guarantee the existence of solution to HJE. Before we move on, an example to calculate the Legendre Transform for a smooth function is described below.

Example 2.4.1 Legendre Transform of $f(x) = x^2$

First we compute the relation between x and s .

$$s = \frac{df}{dx} = 2x \tag{2.35}$$

$$\Rightarrow x = \frac{s}{2} \tag{2.36}$$

Then we use the definition of the Legendre Transform to get,

$$h(s) = \frac{s^2}{2} - \frac{s^2}{4} \tag{2.37}$$

$$\Rightarrow h(s) = \frac{s^2}{4} \tag{2.38}$$

2.4.2 Generalized Legendre Transform

The generalised Legendre Transform is defined for functions having non-differentiable points. The mapping $x \rightarrow \nabla f(x)$ is replaced by a set valued mapping $x \rightarrow \partial f(x)$, where $\partial f(x)$ is the sub-differential of $f(x)$. The formal definition of the Legendre Transform is given by,

Definition 2.4.2 Generalised Legendre Transform

Assume a convex function $f(x)$, where $x \in \mathbb{R}^n$ and $f : \mathbb{R}^n \rightarrow \mathbb{R}$. The generalised Legendre Transform is a mapping defined by

$$f^*(s) = \sup_x \{ \langle s, x \rangle - f(x) : x \in \text{domain}(f) \} \quad (2.39)$$

We now end this section by presenting an example to calculate the Generalised Legendre Transform of a non-differentiable function $f(x) = |x|$.

Example 2.4.2 Legendre Transform of $f(x) = |x|$

Using the definition of the Generalised Legendre Transform,

$$f^*(s) = \sup_x \{ sx - |x| \} \quad (2.40)$$

$$= \sup_x \begin{cases} sx - x & x > 0 \\ sx + x & x < 0 \end{cases} \quad (2.41)$$

$$= \sup_x \begin{cases} (s-1)x & x > 0 \\ (s+1)x & x < 0 \end{cases} \quad (2.42)$$

With this for $f^*(x) < +\infty$, we get a condition that $|s| < 1$. Finally, we obtain the Legendre Transform of $f(x)$ to be,

$$f^*(s) = \begin{cases} 0 & |s| < 1 \\ +\infty & \text{otherwise} \end{cases} \quad (2.43)$$

2.5 Coercivity and Legendre Transform

In this section, we make an important comment on the existence of Legendre Transform. The definition of the Legendre Transform given in the previous section can be expressed in terms of infimum rather than supremum by using the property that $\inf\{A\} = -\sup\{-A\}$. Using this, the definition (2.39) can be written as,

$$g^*(q) = \inf_x \{ \langle q, x \rangle - g(x) \} \quad (2.44)$$

where $g(x) = -f(x)$, and $g^*(q = -k) = -f^*(k = -q)$. (2.44) has an infimum only when $g(x)$ is greater than $\langle q, x \rangle$. Coercivity is the property which characteristics this behavior of g .

Definition 2.5.1 0-Coercive function

A continuous function $f : \mathbb{R}^n \rightarrow \mathbb{R} \cup \{+\infty\}$ which satisfies that $f \not\equiv +\infty$, is said to be 0 Coercive when,

$$\lim_{\|x\| \rightarrow +\infty} f(x) = +\infty \quad (2.45)$$

Definition 2.5.2 1-Coercive function

A continuous function $f : \mathbb{R}^n \rightarrow \mathbb{R} \cup \{+\infty\}$ which satisfies that $f \not\equiv +\infty$, is said to be 1 Coercive when,

$$\lim_{\|x\| \rightarrow +\infty} \frac{f(x)}{\|x\|} = +\infty \quad (2.46)$$

With the definitions of 0 and 1 Coercive functions, we make the following important proposition. The proof of the same is given in [8]

Proposition 2.5.1 *If a function $f : \mathbb{R}^n \rightarrow \mathbb{R} \cup \{+\infty\}$ is 1-Coercive, then $f^*(s) < +\infty \ \forall s \in \mathbb{R}^n$*

This proposition gives us the necessary condition for the Legendre Transform to be well defined. For this we consider two examples to illustrate this proposition.

Example 2.5.1 *The Legendre Transform of $f(x) = |x|$ is given by*

$$f^*(s) = \begin{cases} 0 & |s| < 1 \\ +\infty & \text{otherwise} \end{cases} \quad (2.47)$$

We see that the Legendre Transform is not well-defined for $|s| > 1$. We can readily see from the definition of 1-coercivity that $f(x) = |x|$ is not 1-coercive as,

$$\lim_{|x| \rightarrow +\infty} \frac{|x|}{|x|} = 1 \not\rightarrow +\infty \quad (2.48)$$

On the other hand for the function $f(x) = x^2$, the Legendre transform exists $\forall s$ and is equal to $f^(s) = \frac{s^2}{4}$. We can see that $f(x) = x^2$ is 1-coercive as well.*

2.6 Compatibility Condition

In this section, we study the existence of solution to the Hamilton Jacobi Equation. We formulate a necessary condition for the existence of solution, by imposing a condition on the Boundary data using the Viscosity subsolution Criterion - called the compatibility condition. Using the tools discussed in the previous sections on Legendre Transforms and Coercivity, we define a compatibility condition on the Boundary data in terms of the Legendre Transform. Finally, we present an example that illustrates the compatibility condition for the 1D Eikonal Equation and end this section.

2.6.1 Viscosity Subsolution Criterion

Let $x, y \in \bar{\Omega}$, and $\xi(t) : [0, T] \rightarrow (\xi_1, \xi_2, \dots, \xi_n)^T \in \mathbb{R}^n$ be a Lipschitz continuous path function such that $\xi(0) = x, \xi(T) = y$ and $|\xi'(t)| \leq 1$ a.e $\forall t \in [0, T]$ and u is parametrized by $\xi(s)$.

For the Dirichlet Problem,

$$\begin{aligned} |\nabla u| &= f(\mathbf{x}) & \text{in } \Omega \\ u(\mathbf{x}) &= \varphi(\mathbf{x}) & \text{on } \partial\Omega \end{aligned}$$

using the sub-solution condition, for a convex Hamiltonian, a condition can be derived on $u(x)$ (see [11] for more details).

$$|u(y) - u(x)| \leq L(x, y) \quad (2.49)$$

where,

$$L(x, y) = \inf_{\xi, T} \left\{ \int_0^T f(\xi(s)) ds \ ; \ \xi(0) = x, \xi(T) = y, |\xi'(t)| \leq 1 \text{ a.e in } [0, T] \right\} \quad (2.50)$$

In particular, writing this condition for the boundary data,

$$|\varphi(x) - \varphi(y)| \leq L(x, y) \quad (2.51)$$

gives the compatibility condition. This condition becomes the necessary and the sufficient condition for the existence of solution to the Dirichlet Problem (see [11] for more details).

2.6.2 Compatibility condition using Legendre Transform

In this section, we define the compatibility condition using the Legendre Transform. This result is used to prove the existence of solution to the Prados Model for Shape from Shading which will be discussed in Chapter 4. The compatibility condition in terms of the Legendre Transform is given by,

$$|\varphi(x) - \varphi(y)| \leq L(x, y) \quad (2.52)$$

where,

$$L(x, y) = \inf_{\xi, T} \left\{ \int_0^T H^* \left(\xi(s), -\frac{d\xi}{ds} \right) dx \quad ; \xi(0) = x, \xi(T) = y, |\xi'(t)| \leq 1 \text{ a.e in } [0, T] \right\} \quad (2.53)$$

The constraint $|\xi'(t)| \leq 1$ is imposed to make the Legendre Transform well defined. For example, in the case of the Convex Hamiltonian $H(x, p) = |p| - 1$, the Legendre transform is well defined only if $|s| < 1$. Since the Legendre transform is computed w.r.t the derivative p , the condition is imposed on $\frac{d\xi}{ds}$.

We end this section by providing a short example, illustrating the compatibility condition for a 1D Eikonal equation with DBC.

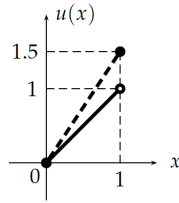
Example 2.6.1 Consider the following Dirichlet Problem,

$$|u'| = 1 \quad \text{on } \Omega = (0, 1) \quad (2.54)$$

$$u(0) = 0 \quad (2.55)$$

$$u(1) = 1.5 \quad (2.56)$$

This problem has no solution, because the slope of $u(x)$ is 1 and at the boundary we have $u(1) = 1.5$.



This means, we cannot find a solution that satisfies this Dirichlet Problem. This can be seen from the compatibility condition defined by (2.50)-(2.51), as

$$|\varphi(1) - \varphi(0)| = 1.5 \geq L(0, 1) = \int_0^1 1 ds = 1 \quad (2.57)$$

which does not satisfy the Compatibility condition (2.51).

2.7 Comparison Theorem

In this last section of the chapter, we study the uniqueness of the solution to the Hamilton Jacobi Equation. We start with the classical comparison principle to illustrate how uniqueness can be proved for classical solutions. We then try to extend it to the viscosity setting to study the uniqueness of the viscosity solution. Ishii[10] in his work presented and proved a comparison principle. Refer[11] for a detailed version for the proof of the comparison theorem.

2.7.1 Classical Comparison Theorem

The classical version of the comparison theorem, involves assuming two distinct solutions u_1 and u_2 solving the PDE, eventually showing that they are equal. This is done by showing that,

$$u_1 \leq u_2, \quad u_2 \leq u_1 \quad \text{in } \bar{\Omega} \quad (2.58)$$

Refer [11] to see how this is done. The procedure followed here does not work for proving uniqueness for non-differentiable solutions like $u(x) = |x|$, as the classical derivatives are no longer defined at points of non-differentiability. To define this in the viscosity setting, we have our new comparison theorem, by Ishii[10].

2.7.2 Comparison Theorem

In this section we state the formal statement of the comparison theorem and see how that is used to conclude the uniqueness of the viscosity solution.

Before we state the theorem, we give the definition of modulus and a couple of Hypothesis on the Hamiltonian H . Consider the following HJE, with an Eikonal type Hamiltonian.

$$H(x, Du(x)) = 0 \quad (2.59)$$

Definition 2.7.1 Modulus: A function $m : [0, \infty[\rightarrow [0, \infty[$ is called a modulus if its continuous and non-decreasing and satisfies $m(0) = 0$

The two Hypothesis (H1) and (H2) on the Hamiltonian are stated below.

1. (H1) There is a modulus m such that

$$|H(x, p) - H(y, p)| \leq m(|x - y|(1 + |p|)) \quad (2.60)$$

for $x, y \in \Omega$ and $p \in \mathbb{R}^n$

2. (H2) The function $p \rightarrow H(x, p)$ is convex on \mathbb{R}^n for each $x \in \Omega$.

Theorem 2.7.1 Comparison Theorem

Let Ω be a bounded open subset of \mathbb{R}^n . Assume that (H1) and (H2) holds. Let \bar{u} and $\underline{u} \in C^0$, respectively be viscosity super- and sub- solutions with

$$\underline{u} \leq \bar{u} \quad \text{on } \partial\Omega \quad (2.61)$$

Also assume that

(H3) \exists a function $\varphi \in C^1(\Omega) \cap C^0(\bar{\Omega})$ such that, $\varphi \leq \underline{u}$ in $\bar{\Omega}$ and

$$\sup_{x \in \omega} H(x, D\varphi(x)) < 0 \quad \forall \omega \subset \subset \Omega \quad (2.62)$$

then $\underline{u} \leq \bar{u}$ in Ω

With this, we have the uniqueness result,

Theorem 2.7.2 *Let u, v be two viscosity solutions of the Eikonal type HJE, such that $u = v$ on $\partial\Omega$. Then $u = v$. Thus, the BVP,*

$$H(x, Du(x)) = 0 \quad \text{in } \Omega \quad (2.63)$$

$$u(x) = \varphi(x) \quad \text{on } \partial\Omega \quad (2.64)$$

has atmost one viscosity solution.

Proof: *The proof is a direct consequence of the comparison theorem. As u and v are both viscosity sub- and super-solutions, by the comparison principle, $u \leq v$ and $v \leq u$ on Ω . This implies $v = u$ on Ω .*

Chapter 3

Orthographic Shape from Shading

3.1 Mathematical formulation of the Model

One of the first attempts to solve this classical inverse problem was by Berthold K.P Horn by finding solutions of nonlinear first order partial differential equation called the *brightness equation* under specific assumptions. This *brightness equation* in simple words can be described as the map between the image intensities to the slope of the unknown surface, so that the shape can be constructed from the shading.

From Figure (6.6), in an orthographic camera model the surface point is directly projected onto the retinal plane in contrast to the perspective model which will be discussed in detail in Chapter 4.

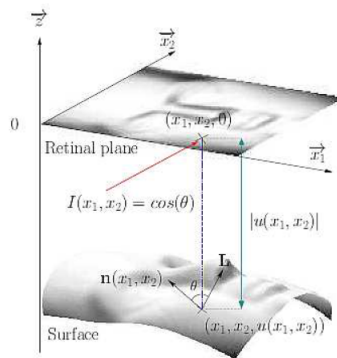


Figure 3.1: Orthographic camera model

The modelling of the problem leads to a partial differential equation. This equation arises from the following

$$I(x_1, x_2) = R(n(x_1, x_2)) \quad (3.1)$$

where (x_1, x_2) are the coordinates of a point x in the image. The brightness equation is the relation between the reflectance map (R) to the brightness intensity (I). Almost all the shape from shading methods assume that the surface is *Lambertian*. In this case, the reflectance map is the cosine of the angle between the light vector $\mathbf{L}(x)$ and the normal vector $\mathbf{n}(x)$ to the surface.

$$R = \cos(\mathbf{L}, \mathbf{n}) = \frac{\mathbf{L}}{|\mathbf{L}|} \cdot \frac{\mathbf{n}}{|\mathbf{n}|} \quad (3.2)$$

Let Ω be an open subset of \mathbb{R}^2 representing the image domain. For example $]a, b[\times]c, d[$. In the Orthographic model we assume the light vector to be constant. We assume the light source to be unique and punctual. For $y \in \mathbb{R}^3$, we denote $\mathbf{L}(y)$ the unit vector representing the light source direction at the point y . If the light source is located at infinity then the light vector field is uniform (i.e. constant). In this case, we denote by $\mathbf{L} = (\alpha, \beta, \gamma)$ with $\gamma > 0$ and $\mathbf{l} = (\alpha, \beta)$.

Let us denote by u the distance of the points in the scene to the camera. Now we have $\mathbf{n}(x) = (-\nabla u, 1)$. The SFS problem is then, given I and \mathbf{L} , to find a function $u : \bar{\Omega} \rightarrow \mathbb{R}$ satisfying the brightness equation

$$\forall x \in \Omega, I(x) = \frac{-\nabla u(x) \cdot \mathbf{l} + \gamma}{\sqrt{1 + |\nabla u(x)|^2}} \quad (3.3)$$

This equation is rewritten, where $p = \nabla u$.

$$H(x, p) = I(x) \sqrt{1 + |p|^2} + p \cdot \mathbf{l} - \gamma \quad (3.4)$$

In our case we have considered a case where $\mathbf{L} = (0, 0, 1)$ to obtain a Eikonal type equation where the function H is called the *Hamiltonian*.

$$H_{Eiko}(x, p) = |p| - \sqrt{\frac{1}{I(x)^2} - 1} \quad (3.5)$$

3.2 Problem of Uniqueness

Now consider the Eikonal equation in 1D,

$$|u'(x)| = 1 \quad x \in (-1, 1) \quad (3.6)$$

$$u = 0 \quad x \in \{-1, 1\} \quad (3.7)$$

The Hamiltonian $H(x, p) = |p| - 1$ where $p = \nabla u$, is a convex function in p . We now show that the solution $u^+(x) = 1 - |x|$ is the viscosity solution to the problem.

Proof: Let $u - \phi$ attain maximum at x_0 . In this case $x_0 = 0$. This means,

$$u(x_0) - \phi(x_0) \geq u(x) - \phi(x) \quad \forall x \in (-1, 1) \quad (3.8)$$

$$\implies \phi(x) - \phi(x_0) \geq u(x) - u(x_0) \quad (3.9)$$

If $x > x_0 = 0$

$$\frac{\phi(x) - \phi(x_0)}{x - x_0} \geq \frac{u(x) - u(x_0)}{x - x_0} \quad (3.10)$$

$$\implies \lim_{x \rightarrow x_0} \frac{\phi(x) - \phi(x_0)}{x - x_0} \geq \lim_{x \rightarrow x_0} \frac{u(x) - u(x_0)}{x - x_0} \quad (3.11)$$

$$\phi'(x) \geq -1 \quad (3.12)$$

If $x < x_0$, we follow the same procedure to get,

$$\phi'(x) \leq 1 \quad (3.13)$$

We get $|\phi'(x)| \leq 1$, which shows that u^+ is a sub-solution to the Eikonal equation. One can verify that u^+ satisfies the super-solution condition as well and thus is a viscosity solution to the problem, which completes the proof.

It is easy to see that, by using the same steps, that $u^-(x) = |x| - 1$ is **not a viscosity solution** if we choose the Hamiltonian $H(x, p) = |p| - 1$, but is indeed a viscosity solution for the Hamiltonian $H(x, p) = 1 - |p|$. Thus the viscosity solution is dependent on the nature of the Hamiltonian we choose, i.e., (concave or convex).

Let us consider the special case where the Eikonal equation is,

$$|\nabla u| = 0 \quad (3.14)$$

This particular PDE presents us with a huge problem of **uniqueness**. This is evident from the sub-solution definition, that

$$H(x, \nabla \phi) \leq 0 \quad (3.15)$$

$$\implies |\nabla \phi| \leq 0 \quad (3.16)$$

which cannot be satisfied for all cases, as $|\nabla \phi| \geq 0$. This particular case is a problem when we consider the numerical solution of the Shape from Shading Model proposed by Rouy and Tourin [18].

Subsolution condition is satisfied as long as $0 < I(x) < 1$, and the uniqueness is lost as soon as $I(x) = 1$. These places where $I(x) = 1$ are called the **singularity points** where *the solution has to specified in order to obtain the relevent solution*.

Chapter 4

Perspective Shape from Shading

In this chapter, we deal with the perspective camera approach to Shape from Shading problems. This approach differs from the Orthographic Approach and can be considered to be a much more realistic approach to shape from shading. In orthographic projection, we assume that the light direction is given by a single vector $\mathbf{L} = (\alpha, \beta, \gamma)$ and that the light rays are parallel to the retinal plane. In perspective projection model, however the light rays are not assumed to be parallel in case of perspective projection. This enables us to reduce the number of singular points in the image. See Figure (4.1)

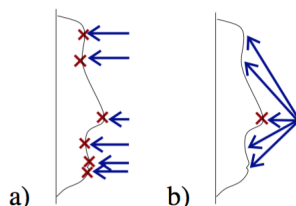


Figure 4.1: a) Orthographic vs b) Perspective : Number of Singular Points

In the perspective projection, the camera can be assumed to be placed at the **focal point**, or at **infinity**. Prados and Faugeras[3] obtained a generic Hamiltonian for a perspective camera approach that unifies these conditions. However, the approach still had the problem of singular points and the information at these points must be specified apriori at these points to single out the unique solution. So, Prados et.al[2] came up with a modified brightness equation to remove the notion of singular points. In this chapter, we discuss the derivation of the HJE that describes the model, and address existence and uniqueness of a viscosity solution.

4.1 Mathematical Model

In this section, we derive the Hamilton Jacobi Equation for perspective model, using the modified brightness equation[2]. Let $\Omega \subset \mathbb{R}^2$. Let the scene be described by a surface \mathbb{S} , which is parametrized

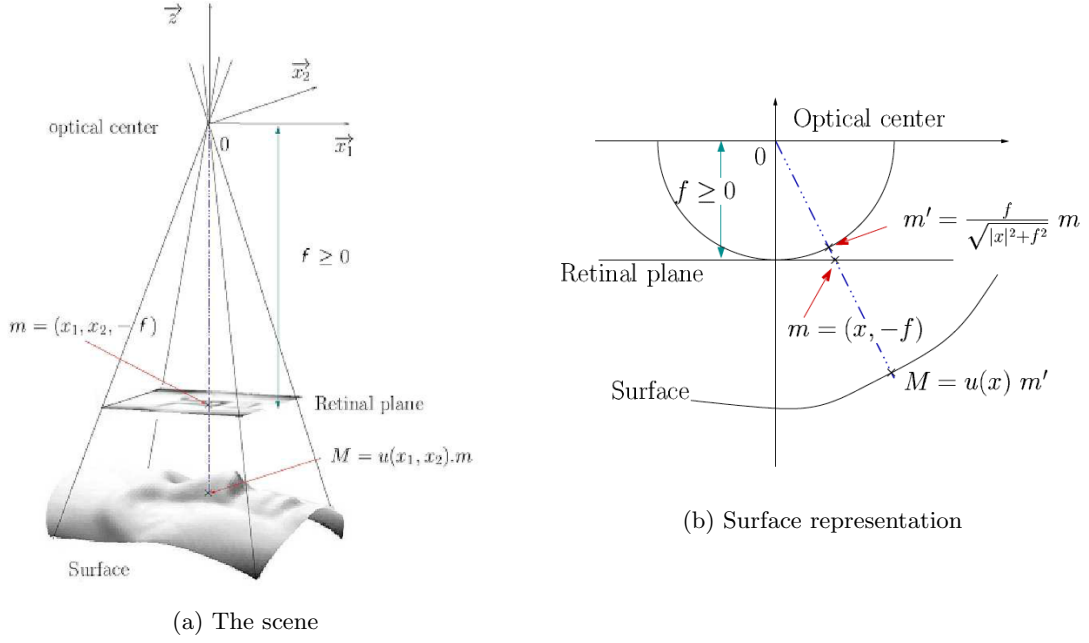


Figure 4.2: Perspective Projection Model

by a function $S : \Omega \rightarrow \mathbb{R}^3$,

$$\mathbb{S} = \{S(x), x \in \bar{\Omega}\} \quad (4.1)$$

Now, let us assume that the light source is placed on the focal point. Figure (4.2a) represents the current setup in a perspective projection model.

From Figure (4.2b), we can deduce that the parametrization of the surface is given by,

$$S(x) = \frac{fu(x)}{\sqrt{|x|^2 + f^2}}(x, -f) \quad (4.2)$$

where f is the focal length of the camera. To simplify the model, Prados et.al in their previous work[3], used the brightness equation

$$R(x) = \cos \theta \quad (4.3)$$

where θ is the angle between the Light Vector and the surface unit normal and $R(x)$ is the irradiance of the surface. This gave a HJE which suffered from singular points. So to overcome this difficulty, Prados et.al[2] did not neglect the $\frac{1}{r^2}$ attenuation term in their model, which would normally be neglected to simplify the model. Contrary to this statement, adding the attenuation term would make the model better posed.

The image irradianace equation (4.3), now becomes,

$$R(x) = \frac{\cos \theta}{r^2} \quad (4.4)$$

where $r = fu(x)$ is the distance between the light source and the considered surface point $u(x)$. Assuming that the surface is lambertian and the camera is placed at the focal point, we have the unit light vector L and the surface unit normal n ,

$$L(S(\mathbf{x})) = \frac{1}{\sqrt{|\mathbf{x}|^2 + f^2}}(\mathbf{x}, -f) \quad (4.5)$$

$$n(\mathbf{x}) = \left(f\nabla u(\mathbf{x}) - \frac{fu(\mathbf{x})}{|\mathbf{x}|^2 + f^2}\mathbf{x}, \nabla u(\mathbf{x}) \cdot \mathbf{x} + \frac{fu(\mathbf{x})}{|\mathbf{x}|^2 + f^2}f \right) \quad (4.6)$$

Using (4.4) - (4.6), and $I(\mathbf{x}) = \cos \theta = L(\mathbf{x}) \cdot n(\mathbf{x})$, we obtain the equation,

$$I(\mathbf{x})f^2 \frac{\sqrt{f^2|\nabla u(\mathbf{x})|^2 + (\nabla u(\mathbf{x}) \cdot \mathbf{x})^2 / Q(\mathbf{x})^2 + u(\mathbf{x})^2}}{u(\mathbf{x})} - u(\mathbf{x})^{-2} = 0 \quad (4.7)$$

Assuming that the surface is visible, that is $u(\mathbf{x}) > 0$, we make a change of variables $v = \ln u$. This gives us the HJE,

$$-e^{-2v} + \frac{I(\mathbf{x})f^2}{Q(\mathbf{x})} \sqrt{f^2|\nabla v(\mathbf{x})|^2 + (\nabla v(\mathbf{x}) \cdot \mathbf{x})^2 + Q(\mathbf{x})^2} = 0 \quad (4.8)$$

where $Q(\mathbf{x}) = \sqrt{\frac{f^2}{|\mathbf{x}|^2 + f^2}}$. (4.8) is the HJE that describes the setting. Solving for $u(\mathbf{x})$ with the known parameters f, I gives the reconstructed 3D object. In the next section, we briefly discuss the existence and uniqueness of the solution to (4.8).

4.2 Existence and Uniqueness

Consider the following Dirichlet boundary value problem,

$$-e^{-2v} + \frac{I(x)f^2}{Q(x)} \sqrt{f^2|\nabla u|^2 + (x \cdot \nabla u)^2 + Q(x)^2} = 0 \quad \text{in } \Omega \quad (4.9)$$

$$u(x) = \varphi(x) \quad \text{on } \partial\Omega \quad (4.10)$$

Let us denote the Hamiltonian of the problem by $H(x, v, p)$, $p = \nabla v$. The following two theorems gives the condition for the existence and uniqueness of solution to the Prados model.

Theorem 4.2.1 *Existence of continuous viscosity solution to the Prados Model*

If

- (A1) **Regularity** : $H \in C^0(\bar{\Omega} \times \mathbb{R}^n)$
- (A2) **Convexity** : H is convex with respect to $\mathbf{p} \ \forall \ \mathbf{x} \in \bar{\Omega}$
- (A3) **Subsolution** : $\inf_{\mathbf{p} \in \mathbb{R}^2} H(\mathbf{x}, u, \mathbf{p}) \leq 0$ in $\bar{\Omega}$
- (A4) **Uniform Coercivity** : $H(\mathbf{x}, u, \mathbf{p}) \rightarrow +\infty$ when $|\mathbf{p}| \rightarrow \infty$ uniformly with respect to $x \in \bar{\Omega}$.
- (A5) $u(\mathbf{x}) = \varphi(\mathbf{x})$ satisfies the compatibility condition.

then u is a continuous viscosity solution of the Hamilton Jacobi Equation.

Theorem 4.2.2 Uniqueness of solution to the Prados Model

If

- (A1) **Convexity** : H is convex with respect to $\mathbf{p} \ \forall \ \mathbf{x} \in \bar{\Omega}$
- (A2) **Space variable regularity** : There exists a modulus m such that $\forall \mathbf{x}, \mathbf{y} \in \bar{\Omega}$ and $\mathbf{p} \in \mathbb{R}^2$,
 $|H(\mathbf{x}, u, \mathbf{p}) - H(\mathbf{y}, u, \mathbf{p})| \leq m(|x - y|(1 + |p|))$
- (A3) **Strict Subsolution** : There exists a strict viscosity subsolution \underline{u} , such that $H(\mathbf{x}, \underline{u}, \mathbf{p}) < 0 \ \forall \ \mathbf{x} \in \Omega$

then there exists atmost one continuous viscosity solution to the HJE such that $u(\mathbf{x}) = \varphi(\mathbf{x})$ on the boundary.

A rigorous proof for existence and uniqueness can be found in [2]. Most of the conditions like convexity and regularity of the Hamiltonian can be easily verified. The most interesting property in the theorem is the subsolution condition. The Hamiltonian $H(x, u, p)$ satisfies the subsolution condition, if

$$\implies \inf_{p \in \mathbb{R}^2} H(x, u, p) \leq 0 \quad (4.11)$$

$$\implies -e^{-2u} + I(x)f^2 \leq 0 \quad \forall \ x \in \Omega \quad (4.12)$$

$$\implies I(x)f^2 \leq e^{-2v} \quad (4.13)$$

$$\implies v \leq -\frac{1}{2} \ln(I(x)f^2) \quad (4.14)$$

(4.14) can be reformulated as

$$\implies v_0 = -\frac{1}{2} \ln(\min_{x \in \Omega} I(x)f^2) \quad (4.15)$$

(4.14) assures that a unique viscosity solution exists to the problem. (4.15) can be supplied as an initial condition to evolution type schemes to ensure convergence of the numerical scheme to the exact solution. The notion of singular points disappear in this case as long as (4.14) is satisfied. This is not assured in other cases[3, 16, 15] because of the absence of the e^{-2u} term in the Hamiltonian and thus the subsolution condition is violated at these points. Thus, this model has a unique viscosity solution that satisfies the HJE in Ω and $\varphi(x)$ on $\partial\Omega$.

In the next chapter, we discuss the numerical schemes used to solve Hamilton Jacobi Equations.

Chapter 5

Numerical Schemes

In this chapter, we discuss some interesting numerical methods to solve the Hamilton Jacobi Equations. First we start off with a brief introduction to Hyperbolic Conservation Laws. In the next section, we discuss some of the numerical techniques to solve Hyperbolic Conservation Laws. In section 3, we discuss the numerical schemes to solve Eikonal Type HJE, with the idea of conservation laws. Next, we discuss the numerical schemes to solve the Perspective Projection Model developed by Prados and Faugeras[2].

5.1 Hyperbolic Conservation Laws

Scalar Hyperbolic Conservation Laws in 1D is represented as

$$u_t + f(u)_x = 0 \quad (5.1)$$

where $f : \mathbb{R} \rightarrow \mathbb{R}$ is a smooth function known as Flux. If u is a smooth function, (5.1) can be written in a non-conservative form,

$$u_t + f'(u)u_x = 0 \quad (5.2)$$

(5.2) when augmented with initial conditions $u(x, 0) = u_0(x)$, can be solved with the **method of characteristics**. This is possible only if f is linear. If f is nonlinear, we have non-smooth solutions even if f and u_0 are smooth. On using method of characteristics, we observe that the characteristics intersect at some point say P. At P the solution u takes multiple values. These points where uniqueness breakdown are known as “shocks”. Thus it becomes insufficient to define the solution with the classical theory. So we are in a point to define “weak solutions” to the PDE. For more details, we refer the reader to [12].

Definition 5.1.1 Weak solution

Let $v : \mathbb{R} \times [0, \infty) \rightarrow \mathbb{R}$, be a smooth function with compact support. A bounded measurable function u is said to be a weak solution to (5.1) if

$$\int_0^\infty \int_{-\infty}^\infty (uv_t + f(u)v_x) dxdt + \int_{-\infty}^\infty uv|_{t=0} dx = 0 \quad (5.3)$$

This is obtained directly by multiplying (5.1) with v and then integrating over $R \times [0, \infty)$. If u is a smooth and satisfies (5.3), then u satisfies (5.1). We can show that the shock propagates with a speed s along the discontinuity where,

$$s = \frac{[f(u)]}{[u]} \quad (5.4)$$

and $[f(u)] = f(u_r) - f(u_l)$ is the jump in $f(u)$ across the discontinuity, $[u] = u_r - u_l$ is the jump in u across the discontinuity. This condition is known as the *Rankine-Hugniot Condition*. This states that, no matter what values u_l and u_r might take, the RH Condition must always be satisfied at the shock.

But for (5.1), we may have more than one solution satisfying the RH-Condition. But only one solution is the physically relevant solution. This is known as the Entropy Solution (Analogous to the viscosity solution defined in Chapter 2). An entropy solution satisfies what is known as the entropy condition, which is defined below.

Definition 5.1.2 Entropy condition for convex flux

A discontinuity propagating with a speed s satisfying the RH condition, satisfies the entropy condition if

$$f'(u_l) > s > f'(u_r) \quad (5.5)$$

which is equivalent to $u_l > u_r$ if f is convex.

Definition 5.1.3 Kruzkov Entropy condition

A discontinuity propagating with a speed s satisfying the RH condition, satisfies the entropy condition if

$$\frac{f(v) - f(u_l)}{v - u_l} > s > \frac{f(v) - f(u_r)}{v - u_r} \quad (5.6)$$

This will hold for any flux function f .

Next, we define the *Riemann Problem*. This will be used to construct the numerical schemes, where local Riemann Problems are solved in a finite volume and then patched up to get the solution to our problem.

A conservation law, together with a piecewise constant data having a single discontinuity is known as a Riemann Problem.

$$u_t + f(u)_x = 0 \quad (5.7)$$

$$u(x, 0) = \begin{cases} u_l & x < 0 \\ u_r & x > 0 \end{cases} \quad (5.8)$$

The solution to the Riemman problem for any flux f is given by[12],

$$u(x, t) = \begin{cases} u_l & x < tf'(u_l) \\ (f')^{-1}\left(\frac{x}{t}\right) & tf'(u_l) < x < tf'(u_r) \\ u_r & x > tf'(u_r) \end{cases} \quad (5.9)$$

5.2 Numerical Schemes for Hyperbolic Conservation Laws

In this section, we see how to develop Finite Difference approximations to Hyperbolic conservation laws. First let us consider the problem,

$$u_t + f(u)_x = 0 \quad \text{in } \mathbb{R} \times (0, \infty) \quad (5.10)$$

$$u(x, 0) = u_0(x) \quad x \in \mathbb{R} \quad (5.11)$$

Now we discretize the x axis by $\{x_{i+\frac{1}{2}}\}$, where

$$x_{i+\frac{1}{2}} = \left(i + \frac{1}{2}\right)h, \quad i \in \mathbb{Z}, h > 0 \quad (5.12)$$

and t by $\{t_n\}$, where

$$t_n = n\Delta t \quad n = 0, 1, 2, \dots \quad (5.13)$$

Let $\lambda = \Delta t/h$. Let v_i^n denotes the approximate solution at the point $(x_{i+\frac{1}{2}}, t_n)$. Thus the initial data $\{v_i^0\}$ is given by

$$v_i^0 = \frac{1}{h} \int_{x_{i-1/2}}^{x_{i+1/2}} u_0(x) dx \quad (5.14)$$

Now, we define the following terms,

Definition 5.2.1 A finite difference scheme is said to be in the conservative form, if there exists a continuous function $F : \mathbb{R}^{2k} \rightarrow \mathbb{R}$ such that

$$v_i^{n+1} = H(v_{i-k}^n, \dots, v_{i+k}^n) = v_i^n - \lambda (F_{i+1/2}^n - F_{i-1/2}^n) \quad (5.15)$$

where $F_{i+1/2} = F(v_{i-k+1}^n, \dots, v_{i+k}^n)$. The function F is called the numerical flux.

Definition 5.2.2 A finite difference scheme is said to be consistent with the conservation law if

$$F(v, \dots, v) = f(v) \quad \forall v \in \mathbb{R} \quad (5.16)$$

For the convergence of a scheme to the entropy solution, Lax-Wendroff theorem[4] says that the scheme must be in the conservative form and consistent. This ensures that the approximate solution v_i^n converges to the entropy solution. For the proof of the theorem, we refer the reader to [4].

5.2.1 The Godunov Scheme

The Godunov Scheme for the numerical solution conservation law defined in (5.10) - (5.11) is given by [4, 12],

$$v_j^{n+1} = v_j^n - \lambda (F_{j+1/2}^n - F_{j-1/2}^n) \quad (5.17)$$

$$\text{where} \quad F_{j+1/2}^n = f(w_R(0, v_j^n, v_j^{n+1})) \quad (5.18)$$

where w_R is the solution to the Riemann Problem.

For a convex flux f , the Godunov Flux is given by,

$$F^G(u, v) = \max(f(\max(u, \theta)), f(\min(v, \theta))) \quad (5.19)$$

and for a concave flux f ,

$$F^G(u, v) = \min(f(\min(u, \theta)), f(\max(v, \theta))) \quad (5.20)$$

where $\theta = \min_{u \in \mathbb{R}} f(u)$. This scheme is stable under the CFL - Condition[12]

$$\lambda \sup_j v_j \leq 1 \quad (5.21)$$

For the detailed derivation of the Godunov Scheme, one can refer [12]. We can show that the Godunov scheme is in the conservative form, is consistent, stable under the CFL condition and hence converges to the entropy solution and is a upwind scheme.[12]

5.2.2 Lax-Friedrich Scheme

For the conservative form of the scheme in (5.17), the **Lax Friedrich** Flux is given by

$$F^{LF}(u, v) = \frac{1}{2} \left(f(u) + f(v) - \frac{1}{\lambda}(v - u) \right) \quad (5.22)$$

The Lax-Friedrich Scheme is consistent and stable under the CFL Condition (5.21). Thus this scheme converges to the entropy solution. But Lax-Friedrich Scheme is not an upwind scheme.

5.3 Godunov Scheme for the Eikonal Equation

In this section, we see how the Eikonal Equation in 1D can be viewed as a conservation law, thus enabling us to use the schemes defined in the previous section.

The Eikonal Equation in 1D is given by,

$$|u_x| = 1 \quad (5.23)$$

To solve this equation, we add a transient term u_t and solve it till the steady state is reached.

$$u_t + |u_x| = 1 \quad (5.24)$$

where $u = u(x, t)$. Now set $v = u_x$. Differentiating (5.24) partially with respect to x , we get

$$\begin{aligned} (u_t)_x + (|u_x|)_x &= 0 \\ \implies (u_x)_t + (|u_x|)_x &= 0 \\ \implies v_t + (|v|)_x &= 0 \end{aligned} \quad (5.25)$$

(5.25) is precisely the conservation law, with $f(u) = |u|$. On using the Godunov scheme defined by (5.17), we have

$$u_i^{n+1} = u_i^n - \Delta t \left(F^G \left(0, \frac{u_i^n - u_{i-1}^n}{h}, \frac{u_{i+1}^n - u_i^n}{h} \right) - 1 \right) \quad (5.26)$$

As $f(u) = |u|$ is a convex function, we can say that

$$F^G(u, v) = \max(f(\max(u, 0)), f(\min(v, 0))) \quad (5.27)$$

This idea can be extended to the 2D case as well. For the Eikonal Equation

$$u_t + \sqrt{\left(\frac{\partial u}{\partial x}\right)^2 + \left(\frac{\partial u}{\partial y}\right)^2} = 1 \quad (5.28)$$

we can use the Godunov Flux to approximate the derivatives along each direction. So the scheme would become

$$u_{i,j}^{n+1} = u_{i,j}^n - \Delta t \left(\sqrt{F^{G_x}(0, D^-x, D^+x)^2 + F^{G_y}(0, D^-y, D^+y)^2} - 1 \right) \quad (5.29)$$

where $D^\pm x$ and $D^\pm y$ denotes the forward and backward differences along x and y respectively. This scheme is consistent, stable under the CFL condition $\Delta t \leq \min(h_x, h_y)$.

This can be extended to the Hamiltonian defined by Prados in [2] as well. The derivatives have to be replaced by the appropriate Fluxes to get the explicit scheme. The second term can be upwinded (D^x and D^y) according to the derivative formula chosen by the Godunov Flux. One can easily verify that the scheme to solve the model is given by,

$$v_{i,j}^{n+1} = v_{i,j}^n - \Delta t \left(-e^{-2v_{i,j}} + J(x_i, y_j) \sqrt{f^2 \left((F^{G_x})^2 + (F^{G_y})^2 \right) + (x_i D^x + y_j D^y)^2 + Q(x_i, y_j)^2} \right) \quad (5.30)$$

The upwinding can be taken one-step further by taking $J(x, y)$ inside the square-root and upwinding $J(x, y)$ along with the derivatives. The results seem to be better when upwinding is done with $J(x, y)$ included inside the square root (Shown in Chapter 6) compared with the standard upwinding. In view of brevity, we just illustrate how the Godunov flux is modified.

$$J_{i,j} F^{G_x}(0, D^+x, D^-x) \implies F^{G_x}(0, J_{i+1,j} D^+x, J_{i,j} D^-x) \quad (5.31)$$

where $J_{i,j} = J(x(i), y(j))$. Similarly upwinding is done in the y direction. The second and the third term is multiplied by $J_{i,j}$ alone.

Chapter 6

Numerical Experiments

In this chapter we present some of the numerical results which we have obtained by using the convergent schemes discussed in the previous chapter. We give the results of the following,

- 1D Eikonal Equation
- Eikonal Equation in 2D.
- Solving Eikonal Equation on non-rectangular domains using the Immersed Boundary method.
- Results of the orthographic projection model.
- Results of the perspective projection model by Prados.

6.1 1D Eikonal Equation

In this section, we present the solution to the most basic Hamilton Jacobi Equation. We use the Godunov Scheme defined in the previous chapter. This scheme converges to the unique viscosity solution, as it is consistent, stable, monotone and the original problem accepts a comparison principle [11]. Figure (6.1) shows the unique viscosity solution $u(x) = 1 - |x|$ to the following Dirichlet Problem.

$$|u'| = 1 \quad \text{in } (-1, 1) \quad (6.1)$$

$$u = 0 \quad \text{on } \{-1, 1\} \quad (6.2)$$

The next figure (Figure (6.2)) shows evolution of the solution to (6.1) - (6.2).

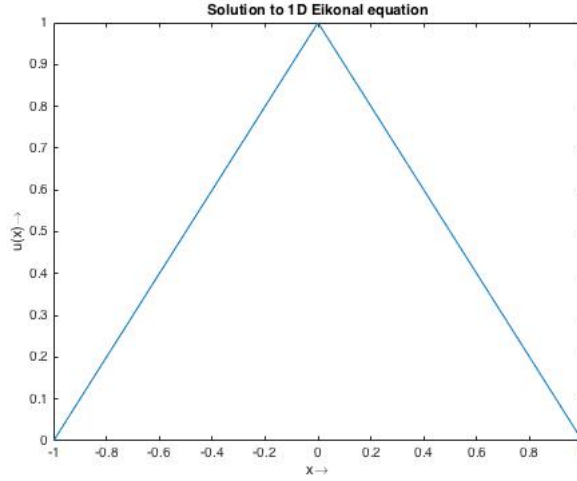


Figure 6.1: Viscosity Soution of the 1D Eikonal Equation

6.2 2D Eikonal Equation

Next, we show the solution to the Eikonal Equation in 2D for a rectangular domain. For this, we have used the Godunov scheme as well, the fluxes approximating the derivatives along each directions.

$$|\nabla u| = 1 \quad \text{in } \Omega = (-1, 1) \times (-1, 1) \quad (6.3)$$

$$u = 0 \quad \text{on } \partial\Omega \quad (6.4)$$

Figure (6.3) shows the solution to the above Dirichlet Boundary Value Problem. We have taken a 50×50 mesh to solve the above problem.

6.3 Immersed Boundary Method for 2D Eikonal Equations

So far, the fintie difference techniques can be easily applied to a rectangular cartesian grid. The objective is to extend the same finite difference techniques to a variety other domains, for example - *Circle, L-Domain, Circle with hole* etc.

To illustrate the technique, we consider a circular domain. For comfort, let us consider a unit circle. We take a rectangular cartesian grid shown in Figure 1.1 and “**immerse**” the circluar domain into the rectangular mesh as shown in Figure 4.1. This technique is known as the immersed boundary method [14] which is widely used to solve problems in Fluid Mechanics.

The first challenge in this method is to track the interior and boundary of the immersed domain. For this we introduce a data structure called the **inout** matrix. The **inout** matrix is defined as

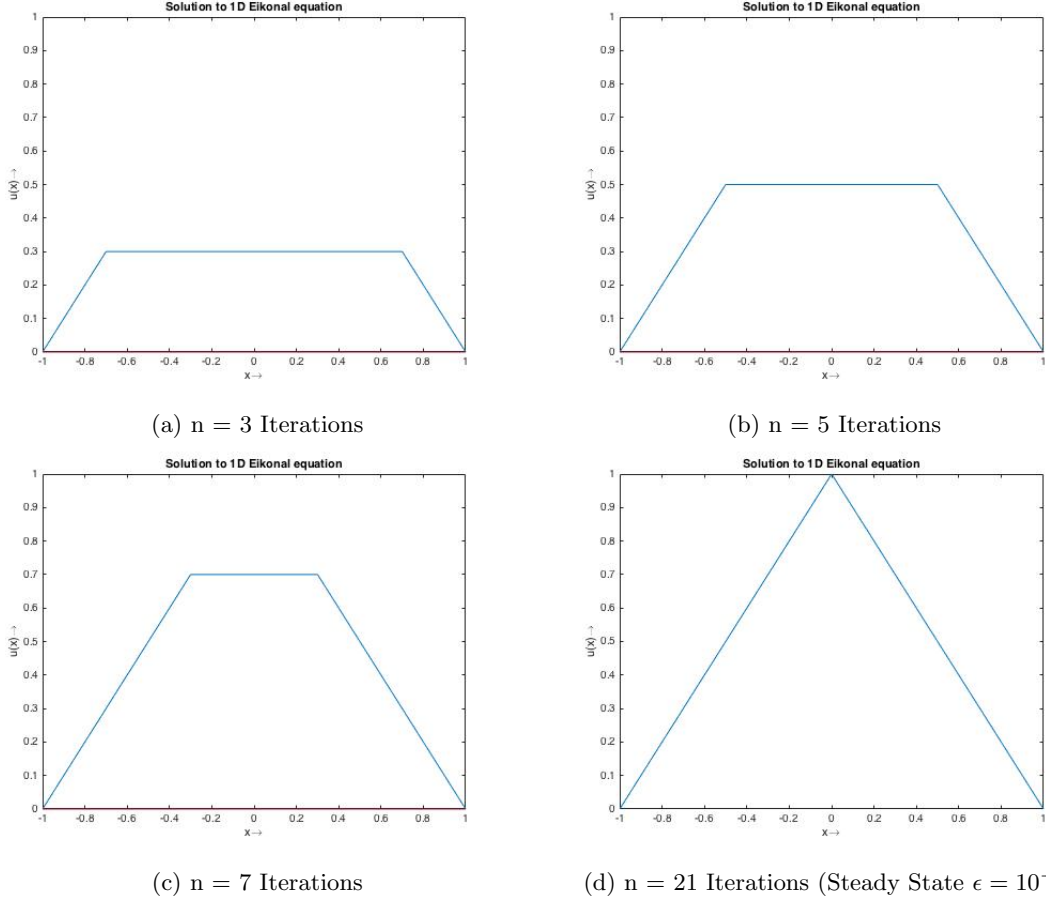


Figure 6.2: Evolution of solution to the Eikonal Equation. The steady state condition is taken as $\|U^{n+1} - u^n\| < \epsilon = 10^{-16}$

follows,

$$inout_{ij} = \begin{cases} 0, & \text{if } (x_i, y_j) \text{ lies inside the immersed domain} \\ 1, & \text{otherwise} \end{cases} \quad (6.5)$$

The way to track the boundary of the immersed domain using the **inout** matrix is natural. We simply ignore the grid points whose **inout** entry is 1 and set the value $u(x, y) = 0$ at those places. We then solve the eikonal equation using only inside the immersed boundary where the **inout** value is 0.

To apply the boundary conditions, we are in a position to obtain the points marked in **red** in Figure 6.4. These points are easily obtained by solving the grid lines $x = -1 + ih_x$ or $y = -1 + jh_y$ with the equation of the circle. Note that, from the Dirichlet boundary condition, the value of $u(x, y)$ is prescribed in the problem at these points.

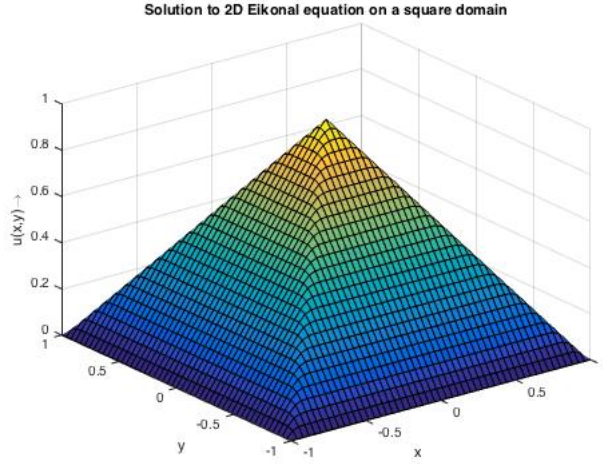


Figure 6.3: Solution of 2D Eikonal Equation

When we apply the finite difference formula on the point which is immediately next to the **red** point - inside the domain, we are in a position to use the distances μ_x and μ_y to calculate the finite differences. This is the place where we choose to ignore the points outside the immersed boundary, and take the points that lie on the circle instead.

With the distances μ_x and μ_y , the update formula near the immersed boundary becomes,

$$v_{ij}^{n+1} = v_{ij}^n - \Delta t \left(\sqrt{D_x^2 + D_y^2} - 1 \right) \quad (6.6)$$

$$D_x = \max \left(\frac{v_{i+1,j} - v_{i,j}}{\mu_1}, \frac{v_{i-1,j} - v_{i,j}}{\mu_2}, 0 \right) \quad (6.7)$$

$$D_y = \max \left(\frac{v_{i,j+1} - v_{i,j}}{\mu_3}, \frac{v_{i,j-1} - v_{i,j}}{\mu_4}, 0 \right) \quad (6.8)$$

where $\mu_{1,...,4}$ is chosen accordingly, depending on the position of top, bottom, left or right neighboring grid points. If the grid point above the current point, lies on the boundary, then $\mu_3 = \mu_y$ and $\mu_1 = \mu_2 = h_x$, $\mu_4 = h_y$ and so on. There may be cases where two of the neighboring grid points may lie on the boundary. All those cases must be taken proper care of. Results of some numerical experiments are shown in the next chapter.

6.3.1 Results

Some Numerical Experiments were carried out using the Godunov scheme for a variety of domains.

Numerical Experiments were conducted using **Fortran90** to find out the order of convergence of the scheme with $\epsilon = 10^{-16} \approx \text{Machine Error}$. The **inout** matrix for a circle with a 10×10 mesh is shown in Figure 6.5

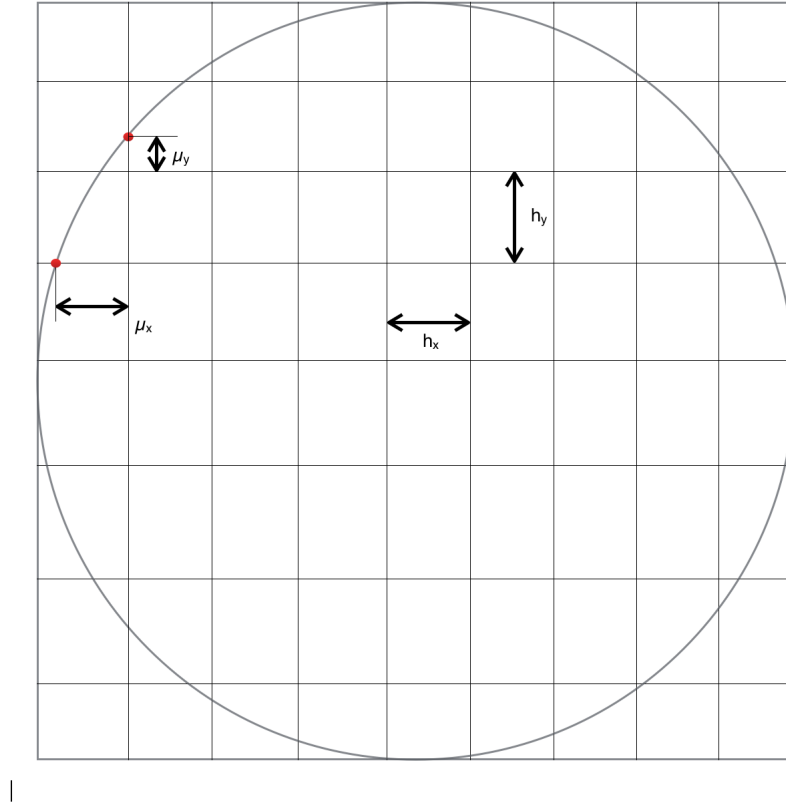


Figure 6.4: Immersed Circle

inout =										
1	1	1	1	1	1	1	1	1	1	1
1	1	1	0	0	0	0	0	1	1	1
1	1	0	0	0	0	0	0	0	1	1
1	0	0	0	0	0	0	0	0	0	1
1	0	0	0	0	0	0	0	0	0	1
1	0	0	0	0	0	0	0	0	0	1
1	0	0	0	0	0	0	0	0	0	1
1	0	0	0	0	0	0	0	0	0	1
1	1	0	0	0	0	0	0	0	1	1
1	1	1	0	0	0	0	0	1	1	1
1	1	1	1	1	1	1	1	1	1	1

Figure 6.5: **Inout** Matrix for 10×10 mesh

With this **inout** matrix, we compute the necessary distances near the boundary, for use in the Finite Difference Formula. Following is the profile, obtained when the Godunov Scheme is run for 50×50 mesh on the master rectangle with steady state $\epsilon = 10^{-16}$.

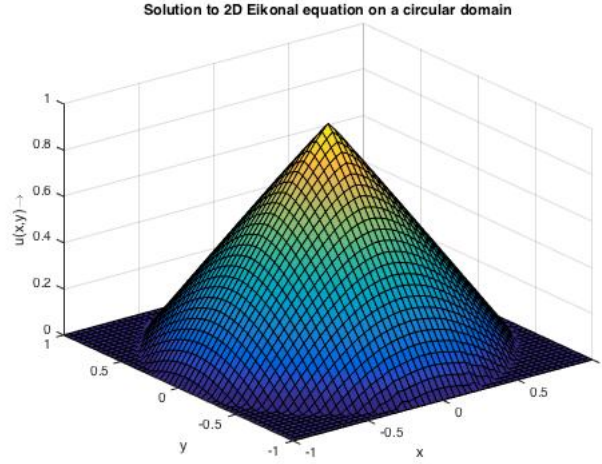


Figure 6.6: Solution in a circular domain

Using **Fortran90**, order of convergence analysis was performed on the scheme and the results are tabulated.

N	Error	Order of Convergence
10	0.9878E-01	0.685
20	0.6145E-01	0.728
40	0.3710E-01	0.738
80	0.2223E-01	0.761
160	0.1311E-01	0.783
320	0.0762E-01	0.800
640	0.0437E-01	-

The same method can be used to generate profiles for a variety of domains as shown. The idea is to tweak the **inout** matrix corresponding to the shape of the domain and appropriately take care of the immersed boundary grid points.

Figure 6.7a and Figure 6.7b shows the profile that is obtained when the Immersed Boundary Technique is applied to solve the Eikonal Equation on a L-Shaped Domain and a circle with a hole in it (non-convex domains) respectively. Similar Experiments can be conducted to model various problems in a variety of domains.

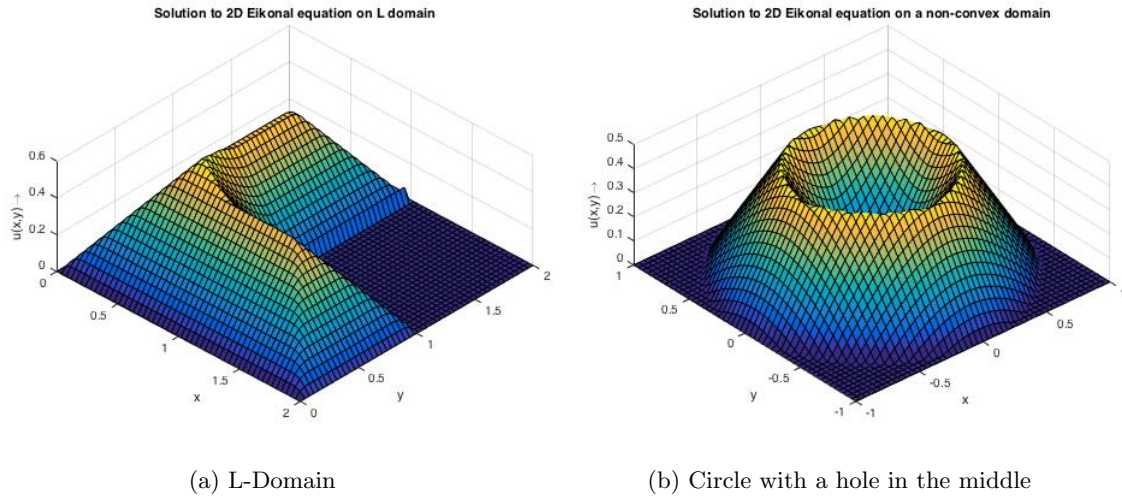


Figure 6.7: Other Domains

6.4 Orthographic Projection

For the orthographic projection model [18], the Eikonal Type HJE, is given by

$$|\nabla u| = \sqrt{\frac{1}{I(x)^2} - 1} \quad (6.9)$$

where $I(x)$ is the intensity function of the input image. Following test was carried out to verify the model using a synthetic image of a vase shown in Figure (6.8).

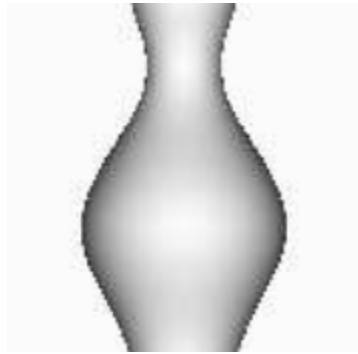


Figure 6.8: Synthetic Test Vase

(6.9) was solved with a Homogeneous Neumann Boundary Condition on $\partial\Omega$ and the result is presented below. The equation was solved using the Godunov upwind scheme.

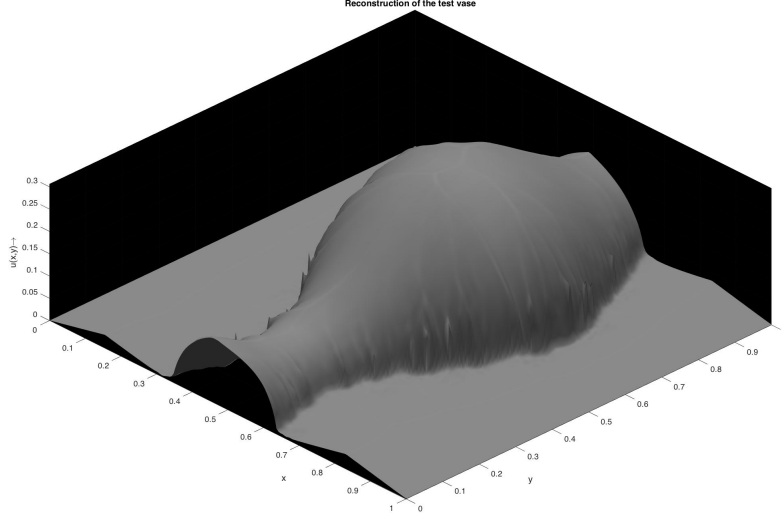


Figure 6.9: Reconstruction of the Synthetic Test Vase

6.5 Perspective Projection Model

The HJE[2] governing the Perspective Projection Model is given by

$$-e^{-2v} + \frac{I(x)f^2}{Q(x)} \sqrt{f^2|\nabla v|^2 + (x \cdot \nabla v)^2 + Q(x)^2} = 0 \quad \text{in } \Omega \quad (6.10)$$

We solve this equation by adding a transient v_t term and then solve till we reach the steady state.

$$v_t - e^{-2v} + \frac{I(x)f^2}{Q(x)} \sqrt{f^2|\nabla v|^2 + (x \cdot \nabla v)^2 + Q(x)^2} = 0 \quad \text{in } \Omega \quad (6.11)$$

To solve the time-dependent problem, we take the constant initial condition

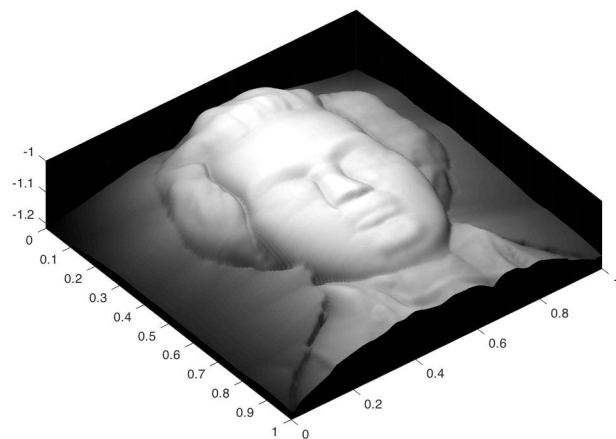
$$v_0 = -\frac{1}{2} \ln(\min_{x \in \Omega} I(x)f^2) \quad (6.12)$$

to ensure convergence to the solution as discussed in Chapter 4. Refer [2] for more details. We used the intensity image and attempted to reconstruct the original 3D shape. The input image along with the reconstructed images are shown in Figure (6.10). Steady State was taken to be $\|U^{n+1} - U^n\| < 10^{-16}$.

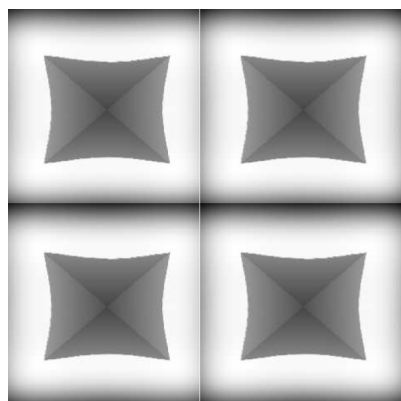
The time evolution of the Mozart Face is shown in Figure (6.11).



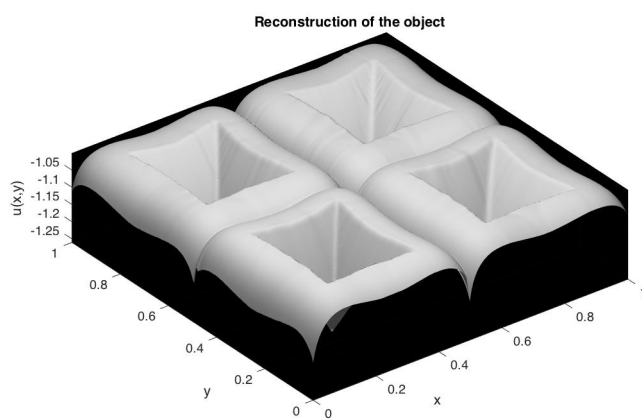
(a) Intensity Image for Mozart



(b) Reconstructed Face of Mozart

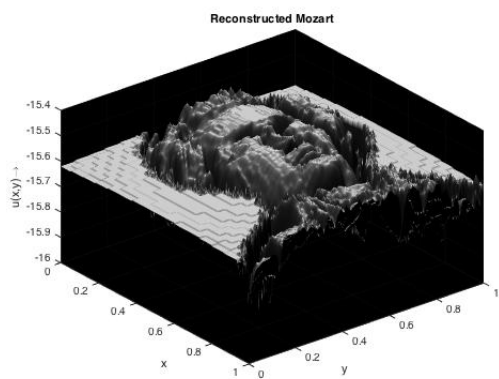


(c) Intensity Image for Test

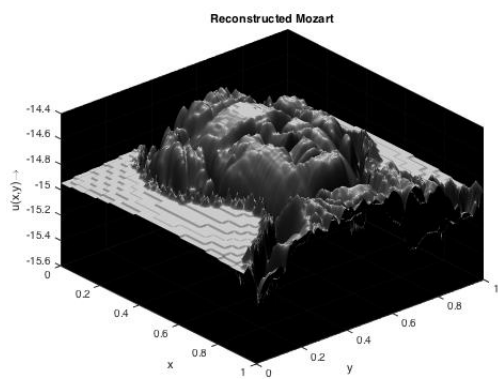


(d) Reconstructed Test Image

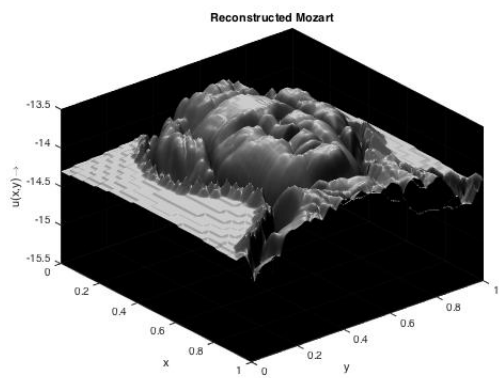
Figure 6.10: Reconstruction using Perspective Model by Prados [2]



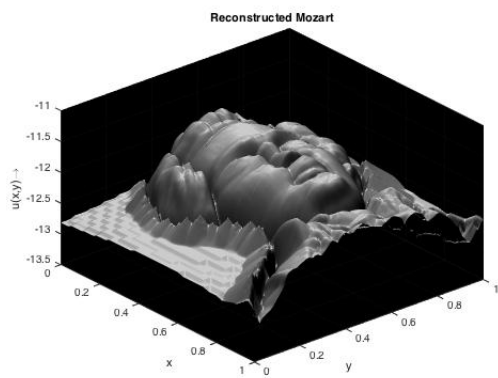
(a) 100 Iterations



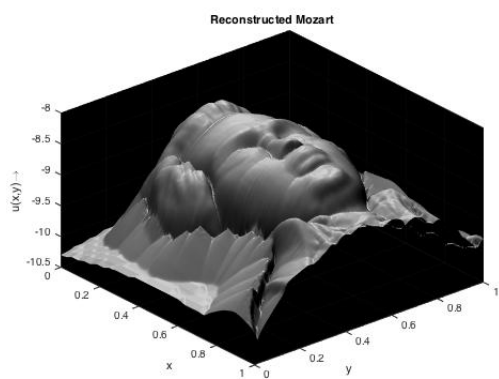
(b) 300 Iterations



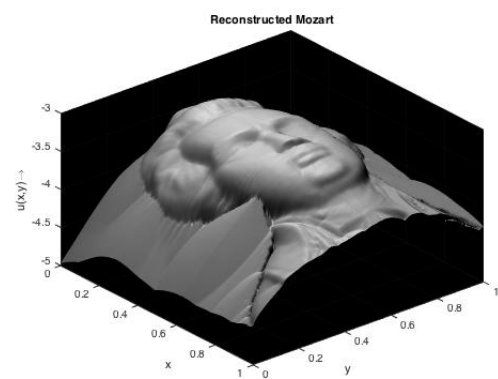
(c) 500 Iterations



(d) 1000 Iterations



(e) 2000 Iterations

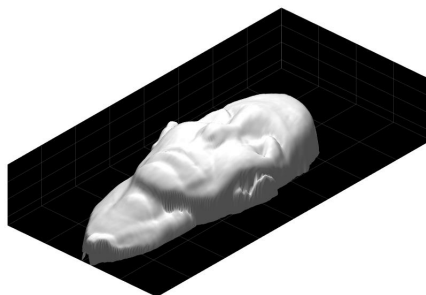


(f) 5000 Iterations

Figure 6.11: Time evolution of Mozart's Face



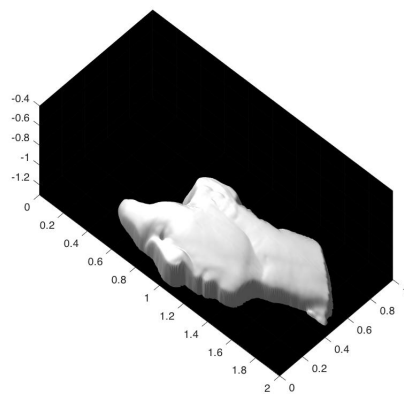
(a) Input Image for Real Face



(b) Reconstructed



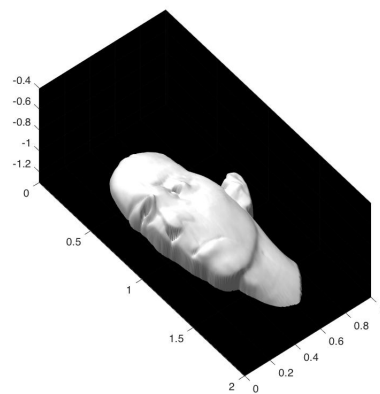
(c) Input image for side view



(d) Reconstructed



(e) Input image for oblique view



(f) Reconstructed

Figure 6.12: Real Life Reconstructions

Chapter 7

Conclusion

So far in this report, we have explored Shape from Shading problems which focus on *lambertian* surfaces, an assumption does not hold for real life objects except for a very few cases. Thus, these models cannot be used for real life applications extensively. But nonetheless SFS has innumerable applications viz. *medical imaging, face reconstruction, terrain mapping, page reconstruction* and so on.

SFS is a simple yet a powerful tool for object reconstruction as it requires minimal input to reconstruct the original scene although the problem becomes difficult for complex cases.

This work can be extended to accomodate the non-lambertian parameters to the Hamilton Jacobi equation in order to get closer to reality. On the other hand analysis namely, existence and uniqueness becomes difficult to study. Also regarding the numerics, one can attempt to develop higher order schemes to improve the accuracy of the solution.

Therefore, there is still room for improvements. It would be very nice if this work has inspired its readers to contribute to the related fields.

For readers who wish to see the code that were used for reconstructions can visit.

<https://www.github.com/Balaje/TIFR.git>

Bibliography

- [1] CRANDALL, M. G., AND LIONS, P.-L. Viscosity solutions of hamilton-jacobi equations. *Trans. Amer. Math. Soc.* 277 (1983), 1-42 (1983).
- [2] EMMANUEL PRADOS, OLIVIER FAUGERAS, F. C. Shape from shading : A well posed problem. Tech. rep., INIRIA, 2004.
- [3] FAUGERAS, E. P. . O. Shape from shading. *Handbook of Mathematical Models in Computer Vision* (2006), 375–388.
- [4] GOWDA, G. Hyperbolic conservation laws, theory and numerics.
- [5] HADAMARD, J. Lectures on cauchy problem in linear partial differential equations. Yale University Press, 1923.
- [6] HAMILTON, W. R. On a generalmethod of expressing the paths of light, and of the planets, by the coefficients of a characteristic function, 1833.
- [7] HAMILTON, W. R. On the application to dynamics of a generalmathematical method previously applied to optics, 1834.
- [8] HIRIART-URRUTY, J.-B., AND LEMARECHAL, C. Convex analysis and minimization algorithms i. *Grundlehren der Mathematischen Wissenschaften, Springer* 305, 1996.
- [9] HORN, B. *Robot Vision*. McGraw Hill Book Company, 1986.
- [10] ISHII, H. A boundary value problem of the dirichlet type forhamilton-jacobi equations. *Annali della Scuola Normale Superiore di Pisa - Classe di Scienze* (1989), 105–135.
- [11] JU, Y. C. Hamilton-jacobi equations for computer vision: Application in shape from shading, 2010.
- [12] LEVEQUE, R. J. Numerical methods for conservation laws.
- [13] OF THE STABILITY OF LINEAR FINITE DIFFERENCE EQUATIONS, S. Peter david lax and robert davis richtmyer. *Communications on Pure and Applied Mathematics*.
- [14] PESKIN, C. S. The immersed boundary method. *Acta Numerica (2002)* (2002), 479517.
- [15] PRADOS, E., AND FAUGERAS, O. A mathematical and algorithmic study of the lambertian sfs problem for orthographic and pinhole cameras. Tech. rep., INRIA, nov 2003.

- [16] PRADOS, E., AND FAUGERAS, O. D. Unifying approaches and removing unrealistic assumptions in shape from shading: Mathematics can help. *ECCV04* (2004).
- [17] R. K. P. ZIA, E. F. R., AND MCKAY, S. R. Making sense of the legendre transform.
- [18] ROUY, E., AND TOURIN, A. A viscosity solutions approach to shape-from- shading. *SIAM Journal on Numerical Analysis* (1992), 867–884.